A MODEL-BASED DESIGN FRAMEWORK FOR ROTORCRAFT TRIM CONTROL LAWS

Carlo E.D. Riboldi, Lorenzo Trainelli, Carlo Capocchiano, Stefano Cacciola
Department of Aerospace Science and Technology, Politecnico di Milano, Milano, Italy

Corresponding author: Carlo E.D. Riboldi, carlo.riboldi@polimi.it

Abstract
Generally speaking, the trim problem is that of finding an equilibrium solution corresponding to an assigned set of well-posed constraints defining the current flight condition of the aircraft. The trim problem appears in different instances in helicopter practice, both in simulation environment and in the field, and analyzing it is a twofold process. Firstly, it is necessary to find an equilibrium condition in terms of rotorcraft states and controls. Secondly, one needs to keep the helicopter in the trimmed condition, which can be accomplished by means of dedicated trim control laws. This paper explores the opportunity to exploit a linearized, airspeed-scheduled high-fidelity model of a helicopter for this twofold task. An analytic linearized model has been defined for hover, feeding the linearized equations of the helicopter dynamics with data obtained from ad-hoc simulations on a detailed multi-body model of a specific testbed, considered also for the testing phase. For higher airspeeds, an approach through model identification has been envisaged for characterizing a suitable system accounting for changes in the dynamics due to forward flight. Subsequently, the models have been used to design control laws based on different strategies, capable of successfully keeping the machine in trimmed flight under various testing conditions. This in turn allows trimming the machine at even higher speeds, thus allowing to identify further models, capturing the dynamics of the system over larger portions of the operating envelope of the rotorcraft. The availability of the linearized model has been fully exploited implementing an automatic procedure for optimal gain tuning, with application to multiple control laws.

1 INTRODUCTION

The problem of trim is a recurring issue in the analysis of rotorcraft flight mechanics. The problem is faced in the existing literature with methods designed to cope both with virtual models of various level of detail, and with the real machine [1], [2].

When working with simple virtual models, capable of simulating only the rigid motion of a rotorcraft, it is possible to use a family of methods based on a direct numerical solution. Such methods attempt to solve iteratively the system of nonlinear equations used for modeling the translational and rotational dynamics of a rigid body, accounting for a forcing effect due to gravity and – for a typical rotorcraft configuration – to the aerodynamics of the main rotor, fuselage, empennages, and tail rotor [3]. The aerodynamics is typically modeled by means of prescribed functions of the kinematic state of the system and of the relative direction of the airspeed.

Similar methods can be profitably used also in presence of the virtual system of equations for the flap and lag dynamics of the rotor, provided these are treated with a suitable harmonic expansion, usually truncated at the first rotor frequency, and hence written in a lumped form based on concentrated parameters, thus without engendering a significant increase in the complexity of the system [3], [4].

A potential issue of this approach is the inaccuracy of the so-obtained trimmed condition. The latter may turn out to be not a trimmed condition for the real helicopter, or not even for a virtual model of the machine built in a higher-fidelity environment, due to the intrinsic limitations of the adopted reduced model.

On the other end, for the trim solution of systems modeled in greater detail, for which explicit equations are too many and impractical to manage, methods known as autopilot-based have been proposed in the past for finding the equilibrium condition. These are based on the idea of controlling the system by means of a suitably designed controller, with the aim of driving all states to a steady flight condition, for assigned values of the airspeed (in terms of both intensity and relative direction) and rotorcraft weight [1]. This approach is suitable for detailed multi-body models including flexible parts, where aerodynamic loads are computed by means of distributed models, such as lifting lines or panels, and it would be ideally suited also for a real helicopter.

This family of methods is clearly more sophisticated to design, and may carry several issues, most notably an instability of the controlled system due to poor characteristics of the controller, and usually implies at least an approximate knowledge of the trim solution before running a trimming simulation. Among the advantages of this technique, there are the greater fidelity of the trimmed condition with respect to the real plant, and the fact that a trimming controller, potentially capable of governing the machine also in presence of disturbances as may happen in flight, is obtained as a side-product of the trim analysis process.

The present paper tries to envisage a common development framework encompassing both trimming techniques, by exploring the mutual connection between the two extreme approaches to the trim problem. In a first stage, a simplified model of a helicopter is recalled, theoretically suitable for approaching the trim problem by means of a numerical integration method [3]. Next, a complete model of the same helicopter is introduced, developed in a high-fidelity multi-body code with fully non-linear, distributed aerodynamics. The equilibrium condition is studied following an autopilot-based approach. The point of contact between the two approaches lies in the use of the reduced, lower-order model to suitably design a controller capable of trimming the higher-order one, thus substantially reducing the difficulty in computing a control law for trimming, with some guarantees on control performance. The trimmed condition obtained by means of this approach, besides being relatively fast to find with respect to other autopilot-based approaches that do not take advantage of the knowledge of the dynamics of the system to be controlled, will be free from the inaccuracies that are potentially present in the trimmed solution obtained from direct integration of the reduced model.

More in depth, in this work two possible ways of exploiting the reduced model for the synthesis of a trimming control law are presented. The first is based on the PID control paradigm, and for that case the reduced model is used to optimally tune the gains in order to satisfy some constraints on the performance of the controlled system. The second makes a more direct use of the knowledge of the dynamics of the system offered by the reduced model, and is based on the design of a model-based linear-quadratic regulator (LQR). Also in that case, an optimization of the weights is carried out making use of the reduced model.

In an effort to cope with the changing dynamics of the system in forward flight at increasing airspeeds, the proposed control design approach can be applied based on a reduced linear model with coefficients scheduled as functions of the airspeed. In order to compute the coefficients of the reduced model at non-null speeds, an identification approach has been proposed where a controller designed for trimming the rotorcraft at a lower airspeed is used at a higher speed – hence in slightly off-design conditions – to find an equilibrium point. Ad-hoc identification analyses are carried out around the new trimmed condition, allowing to identify the dynamics of the system for the corresponding airspeed. This in turn unfolds the potentiality of the proposed approach for a trimming control not limited to the hover condition, but applicable to all airspeeds in the operating envelope of the rotorcraft.

2 THE TRIM PROBLEM

The solution of the trim problem, in mathematical terms, is that of finding the equilibrium point for the non-linear system of equations describing the dynamics of the rotorcraft. In this work, only the rigid motion of a helicopter has been accounted for, whereas the bending and twisting dynamics of the rotor blades has not been included, similarly to the higher-frequency deformation dynamics of more rigid parts of the machine like the fuselage and empennages [3]. The system of non-linear dynamic equations can be formally written as

$$\dot{\boldsymbol{x}} = \boldsymbol{f}\left(\boldsymbol{x}, \boldsymbol{F}_a(\boldsymbol{x}, \boldsymbol{u}), \boldsymbol{F}_g(\boldsymbol{x})\right), \quad (1)$$

where $\boldsymbol{x}$ is the state array, composed of the three linear rates u, v, w, three rotational rates p, q, r, and the attitude angles ϕ, θ, ψ, defined with respect to the longitudinal (roll), lateral (pitch), and vertical (yaw) body axis respectively. The control input array $\boldsymbol{u}$ is composed of the translational motion of the swashplate δ_{sw}, regulating the collective component of blade pitch, the lateral and longitudinal cyclic amplitudes A_1 and B_1 and the rotational speed of the tail rotor Ω_T. The choice of the latter is less typical with respect to tail rotor collective, and it was adopted to cope with a specific design feature of the testbed considered in this work, described in Section 3. The terms $\boldsymbol{F}_a$ and $\boldsymbol{F}_g$ represent the aerodynamic and weight forces respectively.
The arrays of state $\boldsymbol{x}$ and input $\boldsymbol{u}$ can be henceforth arranged in a compact form as

(2) $$\begin{aligned}\boldsymbol{x} &= (u, v, w, p, q, r, \phi, \theta, \psi)^T \\ \boldsymbol{u} &= (\delta_{sw}, A_1, B_1, \Omega_T)^T\end{aligned}.$$

It should be remarked that the forcing term $\boldsymbol{F}_g$ is a function of the three state variables ϕ, θ, ψ only, and not of the other components of the state array.

2.1 Reduced Model for Trim

As mentioned in the introduction, the trim solution of a system of equations such as Eq. (1), which is of relatively small scale, can be found with a direct approach, which usually implies an iterative process, starting from a guess of the solution that will be progressively refined. A typical such algorithm is based on a Newton-Raphson approach, which entails the computation of the sensitivities of the dynamic system to a change in the state and control variables, formally $\left.\frac{\partial f}{\partial x}\right|_{\overline{x},\overline{u}}$ and $\left.\frac{\partial f}{\partial u}\right|_{\overline{x},\overline{u}}$, where $\overline{\boldsymbol{x}}$ and $\overline{\boldsymbol{u}}$ represent the current value of the state and controls in an iteration of the solution algorithm. This process, in turn, allows introducing the linearized system in a natural way. When the values of $\overline{\boldsymbol{x}}$ and $\overline{\boldsymbol{u}}$ have reached convergence to the values $\overline{\boldsymbol{x}}^*$ and $\overline{\boldsymbol{u}}^*$, the latter represent both the equilibrium condition for the non-linear system and, from a strictly mathematical perspective, the reference point of the linearized system, which will be a representation in the vicinity of the equilibrium point of the complete dynamics in Eq. (1).
It is possible to write the linearized system explicitly, starting from the usual form adopted in the literature for the non-linear dynamics of the helicopter. The resulting dynamic equation in matrix form yields

(3) $$\boldsymbol{M}\Delta\dot{\boldsymbol{x}} + \boldsymbol{K}\Delta\boldsymbol{x} + \boldsymbol{L}\Delta\boldsymbol{u} = \boldsymbol{0},$$

where the perturbations are defined as $\Delta\boldsymbol{x} = \boldsymbol{x} - \overline{\boldsymbol{x}}^*$ and $\Delta\boldsymbol{u} = \boldsymbol{u} - \overline{\boldsymbol{u}}^*$. We introduce the terms of the aerodynamic force and CG-centered aerodynamic moments in the local body reference frame,

(4) $$\boldsymbol{F_a} = (X, Y, Z, R_G, M_G, N_G)^T.$$

Matrix $\boldsymbol{M}$ in Eq. (3) can be written as

(5) $$\boldsymbol{M} = \begin{bmatrix} \boldsymbol{M_1} & \boldsymbol{0} & \boldsymbol{0} \\ \boldsymbol{0} & \boldsymbol{M_2} & \boldsymbol{0} \\ \boldsymbol{0} & \boldsymbol{0} & \boldsymbol{M_3} \end{bmatrix},$$

with

(6) $$\boldsymbol{M_1} = \begin{bmatrix} m & 0 & 0 \\ 0 & m & 0 \\ 0 & 0 & m - Z_{\dot{w}} \end{bmatrix},$$

$$\boldsymbol{M_2} = \begin{bmatrix} I_{xx} & -I_{xy} & -I_{xz} \\ -I_{xy} & I_{yy} - M_{\dot{w}} & -I_{yz} \\ -I_{xz} & -I_{yz} & I_{zz} \end{bmatrix},$$

$$\boldsymbol{M_3} = \begin{bmatrix} 1 & 0 & -sin\overline{\theta}^* \\ 0 & cos\overline{\phi}^* & sin\overline{\phi}^* cos\overline{\theta}^* \\ 0 & -sin\overline{\phi}^* & cos\overline{\phi}^* cos\overline{\theta}^* \end{bmatrix}.$$

Here m represents the mass of the helicopter and I_{ij} its inertia moment components in the corresponding indexed plane. The state-sensitivity matrix $\boldsymbol{K}$ in Eq. (3) can be written as

(7) $$\boldsymbol{K} = -\begin{bmatrix} \boldsymbol{K_{11}} & \boldsymbol{K_{12}} \\ \boldsymbol{K_{21}} & \boldsymbol{K_{22}} \end{bmatrix},$$

wherein

(8)
$$K_{11} = \begin{bmatrix} X_u & X_v & X_w & X_p & X_q - m\overline{V}^*\overline{\theta}^* & X_r \\ Y_u & Y_v & Y_w & Y_p + m\overline{V}^*\overline{\theta}^* & Y_q & Y_r - m\overline{V}^* \\ Z_u & Z_v & Z_w & Z_p & Z_q + m\overline{V}^* & Z_r \\ R_u & R_v & R_w & R_p & R_q & R_r \\ M_u & M_v & M_w & M_p & M_q & M_r \\ N_u & N_v & N_w & N_p & N_q & N_r \end{bmatrix},$$

$$\boldsymbol{K_{12}} = \begin{bmatrix} 0 & -mg & 0 \\ mg & 0 & 0 \\ 0 & 0 & 0 \\ & \boldsymbol{0} & \end{bmatrix},\ \boldsymbol{K_{21}} = [\boldsymbol{0} \quad \boldsymbol{I}],\ \boldsymbol{K_{22}} = \boldsymbol{0},$$

g being the intensity of the gravitational acceleration and $\overline{V}^* = \sqrt{\overline{u}^{*2} + \overline{v}^{*2} + \overline{w}^{*2}}$.

Finally, the control-sensitivity matrix $\boldsymbol{L}$ has the form

(9) $$\boldsymbol{L} = \begin{bmatrix} \boldsymbol{L_1} \\ \boldsymbol{0} \end{bmatrix},$$

where

(10) $$\boldsymbol{L_1} = \begin{bmatrix} X_{\delta_{sw}} & X_{A_1} & X_{B_1} & X_{\Omega_T} \\ Y_{\delta_{sw}} & Y_{A_1} & Y_{B_1} & Y_{\Omega_T} \\ Z_{\delta_{sw}} & Z_{A_1} & Z_{B_1} & Z_{\Omega_T} \\ R_{G,\delta_{sw}} & R_{G,A_1} & R_{G,B_1} & R_{G,\Omega_T} \\ M_{G,\delta_{sw}} & M_{G,A_1} & M_{G,B_1} & M_{G,\Omega_T} \\ N_{G,\delta_{sw}} & N_{G,A_1} & N_{G,B_1} & N_{G,\Omega_T} \end{bmatrix}.$$

In order to solve the trim problem, it is necessary to know all coefficients in Eqs. (5), (7) and (9). Except for some of them, depending purely on inertial or kinematic quantities which can be found from the characteristics of the design and assembly of the helicopter of interest, all those expressing sensitivities of the aerodynamic forces and moments with respect to the states and controls need to be obtained someway else.

There are several methods to tackle this problem. The first is trying to find an analytic expression for the sensitivities. To preserve linearity, this implies setting up an analytic aerodynamic model able to capture the dependency of each force component with respect to each state or input in a decoupled way [3], [5].

The sophistication of the aerodynamics of the helicopter in a generic flight condition makes this task very demanding, and the resulting expressions can be difficult to treat and their evaluation error-prone, resulting in an inaccurate numerical description of the dynamics of the system. Nonetheless, for the special case of hover, when the contributions of the fuselage and empennages to the total aerodynamic force are null (neglecting their interaction with the rotor wakes), analytic expressions for the sensitivities in Eqs. (7) and (9) can be derived and are reported in the literature [3]. In hover, each sensitivity is obtained from the sum of two contributions from the main and tail rotor respectively. For many of the sensitivities, the value in hover can be safely assumed null for a helicopter with traditional configuration. This is true also for the two sensitivities $Z_{\dot{w}}$, $M_{\dot{w}}$ in Eq. (6).

With respect to the existing literature, the model considered in Eqs. (1) and (2) shows a difference in the array of controls, where the tail rotor speed Ω_T is used instead of the usual tail rotor collective. The non-null sensitivities which need to be emended are Y_{Ω_T}, R_{Ω_T}, M_{Ω_T} and N_{Ω_T}. The expressions for Y_{Ω_T} and M_{Ω_T}, from which the other two can be easily derived, read respectively

$$Y_{\Omega_T} = \frac{\partial T_T}{\partial \Omega_T}\bigg|_{\overline{\Omega_T}^*} = \frac{\partial}{\partial \Omega_T}\left(\rho A_b \Omega_T^2 R^2 \frac{C_T(\Omega_T)}{\sigma}\right)\bigg|_{\overline{\Omega_T}^*} = \rho A_b \overline{\Omega_T}^* R^2 \left(2\frac{C_T\left(\overline{\Omega_T}^*\right)}{\sigma} + \overline{\Omega_T}^* \frac{\partial\left(\frac{C_T}{\sigma}\right)}{\partial \Omega_T}\bigg|_{\overline{\Omega_T}^*} \right)$$

(11)

$$M_{\Omega_T} = -\frac{\partial Q_T}{\partial \Omega_T}\bigg|_{\overline{\Omega_T}^*} = -\frac{\partial}{\partial \Omega_T}\left(\rho A_b \Omega_T^2 R^3 \frac{C_Q(\Omega_T)}{\sigma}\right)\bigg|_{\overline{\Omega_T}^*} = -\rho A_b \overline{\Omega_T}^* R^3 \left(2\frac{C_Q\left(\overline{\Omega_T}^*\right)}{\sigma} + \overline{\Omega_T}^* \frac{\partial\left(\frac{C_Q}{\sigma}\right)}{\partial \Omega_T}\bigg|_{\overline{\Omega_T}^*} \right)$$

where, similarly to [3], T_T and Q_T are the thrust and torque of the tail rotor, ρ is the density of air, A_b and R the area and radius of the rotor, $C_T(\Omega_T)/\sigma$ and $C_Q(\Omega_T)/\sigma$ the thrust and torque coefficients of the tail rotor normalized on its solidity.

The expressions in Eq. (11) exemplify the structure of most sensitivities [3], and highlight their dependence on the derivatives of purely aerodynamic characteristics of the rotor, $C_T(\Omega_T)/\sigma$ and $C_Q(\Omega_T)/\sigma$, which in turn need to be known from a preliminary aerodynamic characterization of the rotor of interest.

2.2 Solutions of the Trim Problem

As pointed out in the introduction, if a reduced model is available, there are at least two possible ways to exploit it with the aim of finding a trimmed solution.
The first is that of directly solving Eq. (1), which can be typically done iteratively. It should be remarked that the problem of trim presented analytically in the previous subsection is formulated in an underdetermined way, the total number of unknowns – 9 trimmed states and 4 controls – being higher than the number of scalar dynamic and kinematic equations, which is 9. For this reason, 4 parameters should be set in order to correctly set up the problem for a direct solution.
For the application considered in this paper – a trimmed condition in hover or in forward flight – it is possible to set the values of the lateral and vertical speeds, as well as the course angle, to zero – $\overline{v}^* = \overline{w}^* = \overline{\psi}^* = 0$ – and the value of the longitudinal speed $\overline{u}^*$ to zero or to the desired value.
In the direct approach, the reduced model is used to find a solution to the trim problem without the need for a controller. On the other hand, when deploying an autopilot, the system is integrated in closed loop towards an equilibrium point. In this paper we shall focus on this technique. In the proposed framework, the reduced model will be employed side by side with a more detailed, multi-body/FEM model of the helicopter of interest for computing the solution of the trim problem. In order to keep computational time low, the autopilot can be designed and tested first on the reduced model, before trying it on the more sophisticated multi-body/FEM model.
In order to make the system more suited for control purposes, it is possible to write it in a state form starting from Eq. (3), yielding

$$\text{(12)} \qquad \begin{aligned} \Delta\dot{\boldsymbol{x}} &= -\boldsymbol{M}^{-1}\boldsymbol{K}\Delta\boldsymbol{x} - \boldsymbol{M}^{-1}\boldsymbol{L}\Delta\boldsymbol{u} \\ &= \boldsymbol{A}\Delta\boldsymbol{x} + \boldsymbol{B}\Delta\boldsymbol{u} \end{aligned}.$$

An eigenvalue analysis can be carried out preliminarily on the state matrix $\boldsymbol{A}$, in order to check the degree of stability of the free dynamic response of the system. This allows assessing the level of criticality of the design of the control system. In the following two subsections, two control architectures exploiting the reduced model in the design process will be presented.

2.2.1 Optimized PID Control

A first control law for trim has been designed based on multiple SISO loops [2], [6], [7]. In order to facilitate the design of the corresponding control laws, the dynamics of the system have been arranged in two layers, as highlighted in Figure. This control scheme is particularly suited for hover or low-speed forward flight.
The internal layer, in red on Figure 1, is a stabilization layer for the faster dynamics of the system. These include the states w and r, controlled with δ_{sw} and Ω_T respectively by means of proportional-integral (PI) control laws. The other fast dynamics in the system are those of the attitude angles ϕ and θ, governed by means of the two cyclic pitches A_1 and B_1. These are controlled through proportional-derivative (PD) control laws, where the derivative term is necessary to obtain a damping effect on the corresponding two states. The potential noise increase in the control input, bound to the feedback of a derivative term, is addressed with a suitable low-pass filter ahead of the derivative gain. The breakdown of the PD control block is shown in Figure 2 for the case of the ϕ-to-A_1 loop.

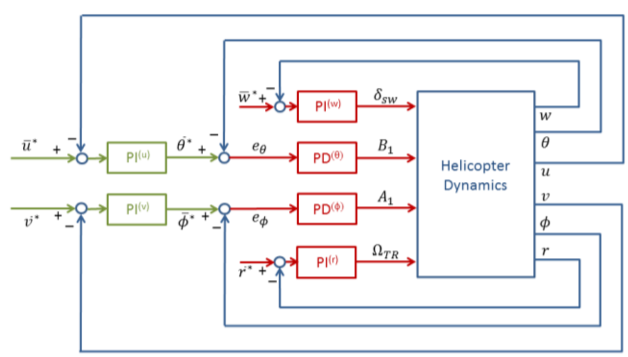

Figure 1: Adopted scheme for the PID controller for trim

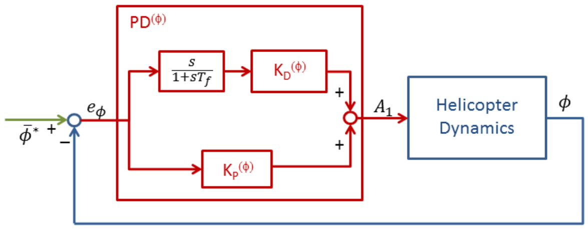

Figure 2: Adopted scheme for PD controllers with filter. Example on ϕ-to-A$_1$ loop.

The reference for the internal layer is either set by the user – for w and r – or obtained from the external layer, in green on Figure 1. This implements two parallel PI loops, working on the longitudinal and lateral speeds u and v, for which the set-point has been set by the user. The two control laws produce the reference values for the states ϕ and θ as control inputs.
It can be noticed that the overall architecture of the system does not take explicitly into account the two rates p, q and the ψ angle. For a trimmed condition in hover or forward flight where all rates are null, sufficient information on those two rates is present in the control architecture through the derivative term in the PD control laws, applied to ϕ and θ. Similarly, information on the yaw angle ψ is accounted for by means of the integral term in the PI loop for the yaw rate r.
In analytical terms, the implementation adopted for the generic PID law can be written in the Laplace domain as

(13) $$PID(s) = k_c\left(1 + \frac{1}{sT_I} + \frac{sT_D}{1+sT_f}\right).$$

The filtering effect on the derivative term can be obtained by tuning the term T_f properly [6]. Considering all control loops in Figure, the array of parameters to be tuned is composed of $\left(k_c^w, T_I^w, k_c^r, T_I^r, k_c^\phi, T_D^\phi, k_c^\theta, T_D^\theta, k_c^u, T_I^u, k_c^v, T_I^v, T_f\right)$.
For simplicity, a single value of T_f has been assumed for both control loops with a derivative term.
To tune the control system, an analysis of the performance by means of the root locus has been adopted first. To this aim, the following equations have been added to the system in state form, Eq. (12), defining the integral terms (subscript 'I') and the dynamics of the filtering action on the errors e_f^ϕ and e_f^θ, yielding

(14) $$\begin{cases} \Delta\dot{r}_I = \Delta r \\ \Delta\dot{u}_I = \Delta u \\ \Delta\dot{v}_I = \Delta v \\ \Delta\dot{w}_I = \Delta w \\ \dot{e}_f^\phi = -\frac{1}{T_f}\left(\Delta\phi + e_f^\phi\right) + \frac{1}{T_f}\Delta\phi_{ref} \\ \dot{e}_f^\theta = -\frac{1}{T_f}\left(\Delta\theta + e_f^\theta\right) + \frac{1}{T_f}\Delta\theta_{ref} \end{cases}.$$

Referring again to the system in Eq. (12), the so-obtained augmented system is based on the augmented arrays of state and control input, defined as

(15) $$\begin{aligned} \Delta\boldsymbol{x}_{aug} &= \left(\Delta\boldsymbol{x}^T, \Delta r_I, \Delta u_I, \Delta v_I, \Delta w_I, e_f^\phi, e_f^\theta\right)^T \\ \Delta\boldsymbol{u}_{aug} &= \left(\Delta\boldsymbol{u}^T, \Delta\phi_{ref}, \Delta\theta_{ref}\right)^T \end{aligned}.$$

Based on these, the control law can be written as

(16) $$\Delta\boldsymbol{u}_{aug} = -K_{PID}\Delta\boldsymbol{x}_{aug},$$

where matrix $\boldsymbol{K}_{PID}$ is a 6-by-15 sparse gain matrix, with the values of proportional, derivative and integral gains as specified by the adopted control scheme (Figure). Substituting Eq. (16) in Eq. (12), augmented with Eq. (14), it is easy to define the state matrix of the controlled system based on a reduced representation of the latter, and computing the eigenvalues for changing values in matrix $\boldsymbol{K}_{PID}$.
Due to the high number of parameters to be tuned for this control law – totaling 13 –, manual tuning is impractical. For the testbed considered in this work, a first manual tuning based on the rules of Tyreus-Luyben has allowed the setup of a stabilizing first guess gain matrix. The root loci associated to each non-null component of $\boldsymbol{K}_{PID}$ have been studied, and the values of the gains have been set correspondingly. Based on the analysis of the root loci, the desired performance of the controller has been negotiated to yield

- a settling time (to within 1% of the set-point) of all dynamics T_{a1}< 4 s;
- a minimum damping of all second order dynamics ζ_{min} > 0.707;

- for the vertical, lateral and longitudinal dynamics the maximum frequency ω_{max}< 6 rad/s, in order to avoid coalescence with rotor frequencies (not accounted for in the reduced model), whereas ω_{max}< 20 rad/s for directional dynamics.

To ease gain tuning, the availability of a linearized reduced system can be exploited further, by setting up an optimization algorithm for the gains. A merit function can be set up considering two key performance parameters which are obtained for an assigned control gain matrix, in the form of $\bar{\zeta}_{min}$, the minimum of all damping factors of the oscillatory modes of the system, and $\bar{\tau}_{max}$, the time constant of the slowest mode in the system. The distances of these two quantities from their respective desired values ζ^* and τ^* define the merit function

(17) $$J_G(\bar{\zeta}_{min},\bar{\tau}_{max}) = \left(\frac{\bar{\zeta}_{min}-\zeta^*}{\zeta^*}\right)^2 + \left(\frac{\bar{\tau}_{max}-\tau^*}{\tau^*}\right)^2.$$

The optimization variables may be in principle all the 13 tuning parameters introduced previously. Due to the limited effect of their change on the dynamics of the system, $(k_c^w, T_I^w, k_c^r, T_I^r)$ can be excluded from the set of optimization variables. In order to compute the merit function, it is necessary to compute the eigenvalues of the controlled system – this is very practical thanks to the available reduced model. Due to the good regularity of the problem, an unconstrained gradient method can be profitably deployed to solve this optimization.

2.2.2 Linear-Quadratic Regulator (LQR)

The linearized reduced model constitutes a necessary asset to start with the synthesis of a model-based control. In this work an LQR optimal control law is considered [8]. The matrices of the linearized system in Eq. (12) can be fed to a numerical solver of the algebraic Riccati equation (ARE), producing in a first stage a purely proportional controller. From a theoretical standpoint, the so-obtained control solution minimizes the functional

(18) $$J = \frac{1}{2}\int_0^\infty (\Delta\boldsymbol{x}^T\boldsymbol{Q}\Delta\boldsymbol{x} + \Delta\boldsymbol{u}^T\boldsymbol{R}\Delta\boldsymbol{u})dt.$$

For the solution process of the ARE it is necessary to specify the diagonal weight matrices $\boldsymbol{Q}$ and $\boldsymbol{R}$ corresponding to the state and input arrays respectively. The control solution obtained through this design algorithm guarantees the asymptotic stability of the dynamics of the controlled system, provided the couple $(\boldsymbol{A},\boldsymbol{B})$ is stabilizable and $(\sqrt{\boldsymbol{Q}},\boldsymbol{A})$ is detectable, which is the case for the considered system (helicopter) and controls, for a wide range of coefficients in $\boldsymbol{Q}$.

A relevant advantage of this algorithm for control design is the automatic and computationally light production of a stabilizing gain matrix $\boldsymbol{K}_{LQR}$, which comes in a closed form from the solution of the associated ARE. Being fed with a detailed description of the dynamics of the controlled system, the so-obtained gains will involve all states and controls, taking into account all couplings, fully exploiting the knowledge of the model physical behavior.

Considering the application to the trim problem, the ability to compute the steady state control values to keep the helicopter in a trimmed condition is a fundamental requirement. This ability cannot be guaranteed by a purely proportional controller. For this reason, it is necessary to augment the array of measurements with integral states.

The inclusion of integral states in the state equation can be easily done *a posteriori* with respect to the formulation of the dynamics of the system. The system with augmented state and control matrices is structured as follows:

(19) $$\begin{Bmatrix}\Delta\dot{\boldsymbol{x}}\\ \Delta\dot{\boldsymbol{x}}_I\end{Bmatrix} = \begin{bmatrix}\boldsymbol{A} & \boldsymbol{0}\\ \boldsymbol{H} & \boldsymbol{0}\end{bmatrix}\begin{Bmatrix}\Delta\boldsymbol{x}\\ \Delta\boldsymbol{x}_I\end{Bmatrix} + \begin{bmatrix}\boldsymbol{B}\\ \boldsymbol{0}\end{bmatrix}\Delta\boldsymbol{u}.$$

Matrix $\boldsymbol{H}$ in Eq. (19) is included to select which states in the original state array are integrated. It is a binary matrix, with as many rows as the number of integrated states and columns as the number of original states.

For the trim problem, the quantities to be integrated are chosen as u, v, w. Once integrated, from a physical standpoint, these provide to the controller a rough knowledge of the drift from its original position. As pointed out, the presence of these states is relevant for it guarantees a null steady state error on the speeds, thus returning the corresponding trim value of the control inputs at the end of the transient.

Similarly to the PID control system, it is necessary to tune the LQR properly to obtain the desired response. Due to the high number of parameters to be tuned, an automatic optimal tuning procedure can be envisaged, based on the same merit function introduced in Eq. (17). Here the optimization is initialized by tuning the weights based on the values of maximum acceptable values for the states and controls $x_{i,max}$ and $u_{i,max}$ [8], yielding a definition of the weight matrices as

$$\boldsymbol{Q} = diag\left\{\frac{1}{x_{i,max}^2}\right\}, \quad \boldsymbol{R} = diag\left\{\frac{1}{u_{i,max}^2}\right\}. \tag{20}$$

The values of $u_{i,max}$ can be assigned based on maximum allowed main rotor swashplate displacements and tail rotor speed, whereas the values of $x_{i,max}$ can be guessed. The corresponding optimization problem will consider $x_{i,max}$ as optimization variables. These can be reduced from 12 to 8 by dropping the parameters corresponding to Δw and Δr and their respective integrals, which have little effect on the value of the merit function.
A comparison between the PID and LQR controllers will be provided in the results.

2.3 Control Scheduling

The use of a reduced model describing the linearized dynamics of the system enables an easier synthesis of controllers based on multiple design algorithms, as shown in the previous paragraphs. By constitution, a linearized system for a given airspeed condition is a good approximation of the real dynamics only in a limited range of speeds around the reference. In particular, the intensity of coupling effects changes substantially as a function of the airspeed, making the response of the helicopter very different over the speed envelope. For this reason, it is crucial to design the control system accounting for a correct representation of the dynamics for each assigned airspeed.
In principle, this can be done in the proposed linear framework by introducing a scheduling of the parameters of the reduced model. In this work we consider two ways to cope with this necessity.
The first, already mentioned in Section 2.1, is that of adopting definitions obtained from a simple characterization of the sensitivities of the system, yielding analytic expressions for the various coefficients in terms of basic quantities characterizing its aerodynamics and inertia. A relevant shortcoming of this approach is that the mentioned analytic dependencies are expressed in terms of several aerodynamic derivatives, not easy to obtain unless exploiting dedicated experiments in a virtual environment or in a wind tunnel, making the procedure prone to inaccuracies. Easier expressions can be obtained from the literature only for the specific case of hover [3], as already pointed out.
A second approach is that of parameter identification. This is based on the idea of studying the response of a sophisticated simulator or a real system starting from a trimmed condition and subjecting it to an assigned history of controls. The time histories of all measured states of interest and of the assigned inputs can be fed to an identification routine, capable of returning the matrices of the linearized system matching the histories of the measured outputs.
For the particular problem of interest here, given the availability of an analytic linearized model for hover, it is possible to envisage a procedure where:

1. a PID or a LQ controller is synthesized for hover based on the analytical model, as explained previously;
2. the controller is applied to the complete, i.e. not reduced, model of the system in slightly off-design conditions (for instance with an airspeed of 10 m/s, using the controller designed for hover) and the trimming controls and attitude are found;
3. starting from the trimmed condition, the complete model is subjected to histories of controls suited for identification, and a corresponding linearized model is identified;
4. a new controller is synthesized, based on the model obtained from step 3.

Steps 2, 3 and 4 can then be repeated to cover the airspeed envelope of the helicopter, finding the trimming controls and attitude for increasing airspeeds. The choice of the airspeed increments depends on the intensity of the related non-linear effects on the dynamics of the system: a loose discretization will cause poor control performance in off-design conditions, corresponding to an increased airspeed.

2.3.1 Identification of a Reduced Model

The problem of model identification on helicopters is made complicated by the inherent instability of the dynamics of these systems, especially at low airspeeds. Several customized procedures have been proposed in the literature, dealing with the particular features of the respective testbeds, especially for hover [9], [10], [11]. After some preliminary investigations in a virtual environment, the helicopter considered in the present study has been deemed unsuitable for open-loop identification procedures, due to instability issues showing up very quickly, even for very small perturbations of a trimmed condition. An identification procedure based on closed-loop simulations has been adopted instead. Here the system is kept under control with an assigned gain matrix, and an additional prescribed perturbation input is introduced on all channels.
In analytical terms, the linearized form of the system to be identified can be written starting from Eq. ((**12**) as

$$\dot{\boldsymbol{x}} = (\boldsymbol{A} - \boldsymbol{BK})\boldsymbol{x} + \boldsymbol{B}\boldsymbol{u}_{id}, \tag{21}$$

where $\boldsymbol{u}_{id}$ is the additional exogenous input introduced for identification. Thanks to the fact that the gain matrix $\boldsymbol{K}$ is known, it is possible to set up a prediction-error method (PEM) algorithm aimed at the identification of $\boldsymbol{A}$ and $\boldsymbol{B}$ from simulations where all states are measured and the time histories of $\boldsymbol{u}_{id}$ are known. This algorithm has been preferred to subspace methods for it allows to specify a structure for the matrices to be identified, thus exploiting all available information and reducing the number of parameters to be computed.
By analyzing the structure of the system matrices for the helicopter case, it is easy to find that the number of unknown parameters is 60. Of these, 36 come from the fully populated block of $\boldsymbol{A}$ linking the states u, v, w, p, q, r to their derivatives, whereas 24 are from the top block of matrix $\boldsymbol{B}$, regulating the input of all four controls into the equations for the components u, v, w, p, q, r of the array of states. All other coefficients in the system matrices are either zero, known *a priori*, or they can be computed offline before identification. The presence of the integral states mentioned in Section 2.2.2 does not increase the number of unknown parameters, for matrix $\boldsymbol{H}$ in Eq. (**19**) is assigned *a priori*.

3 RESULTS

A light helicopter featuring an innovative 2-bladed homokinetic main rotor designed by an industrial partner has been selected as a testbed for all analyses introduced in the previous sections [12], [13], [14], [15]. Another specific feature of this helicopter is the yaw control, which is obtained changing the speed of the fixed-pitch tail rotor, instead of the usual collective pitch at constant speed. A very detailed virtual multi-body/FEM model of the helicopter was assembled in the Cp-Lambda environment, based on [16], taking into account blade flexibility, detailed kinematics of both the hub and the swashplate, 10-state Peters-He dynamic inflow of the main rotor and aerodynamic characteristics of all parts of the vehicle, including the fuselage. The model can be controlled via a control library, receiving control parameters such as reference values and gains as inputs.
The control design framework, including the optimization of the gains, has been assembled in Matlab®, exploiting general-purpose built-in functions for the solution of optimal problems – with application to gain tuning and model identification –, and of the Riccati equation. A PEM identification routine specifically tailored to the form of the considered system was implemented anew in Matlab®.

3.1 Control in Hover

The first results are illustrated through an analysis of the eigenvalues of the system in hover. These results have been obtained after assembling the linearized model for hover, based on the literature [3]. The analytic model was emended considering the specific tail control, and complemented with gradients for C_T/σ and C_Q/σ of both rotors obtained from ad-hoc simulations run on the multi-body model as required by the formulation.

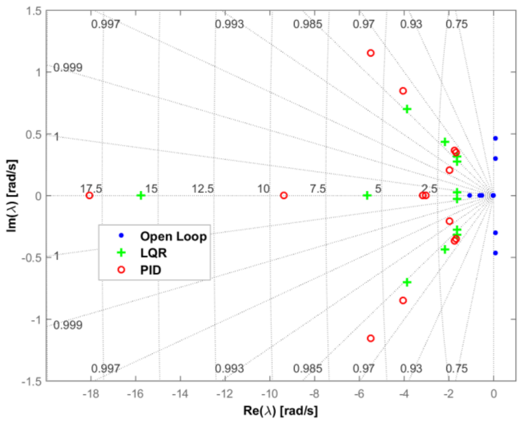

Figure 3: Poles of the linearized system in hover; comparison of open loop (blue) and closed loop (red, PID, and green, LQR) conditions.

3.1.1 Preliminary Control Check

The plot in Figure shows the eigenvalues of the open loop system, compared to those of the controlled system, obtained using a PID and an LQR controller.
The corresponding controllers have been tuned based on the linearized model for hover, applying the model-based optimal tuning of the control parameters described in Sections 2.2.1 and 2.2.2.
The performance of both controllers is quite similar, and both prove capable of stabilizing the system.
A further preliminary validation of the controllers comes from the analysis of the dynamic response on the linearized system used for control design. In Figure , the results of simulations performed on the reduced model for hover are shown for a non-homogeneous initial condition. The results of the optimized PID and LQR are compared.
The time response is similar for the two controllers, and, having a similar performance, it should be remarked that:

1. The LQR law is easier to tune, as a result of the physical meaning of the tuning parameters.
2. The numerous couplings in the system are effortlessly accounted for by the LQR approach. Differently from the PID, a physical knowledge of the dynamics of the system is not necessary to suitably tune the controller.

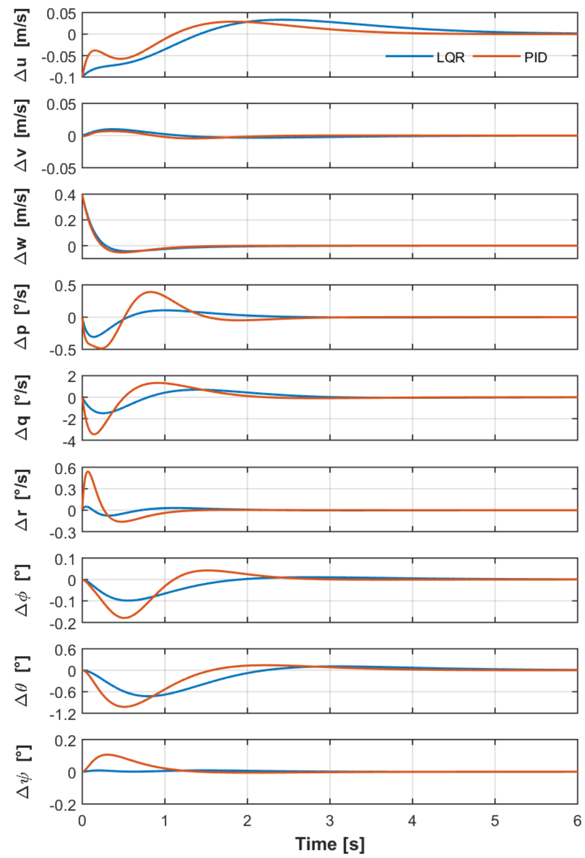

Figure 4: Response of the linearized system in hover to a non-homogeneous initial condition; comparison of PID (red) and LQR (blue) performance.

3. Differently from the LQR, the PID law need to be carefully tuned to ensure closed-loop stability of the response.
4. The control action can be effortlessly limited via dedicated tuning parameters in the LQR case – weights in matrix $\boldsymbol{R}$ –, thus preventing unrealistic control demands and saturation of the actuators.

3.1.2 Trimming the Complete Model

The same cases considered for Figure have been simulated on the complete multi-body/FEM model of the helicopter. Results are shown in Figure 5. In this case the control input tend to non-null values, representing the reference values typical of the new trimmed condition. Also the attitude angles reach an

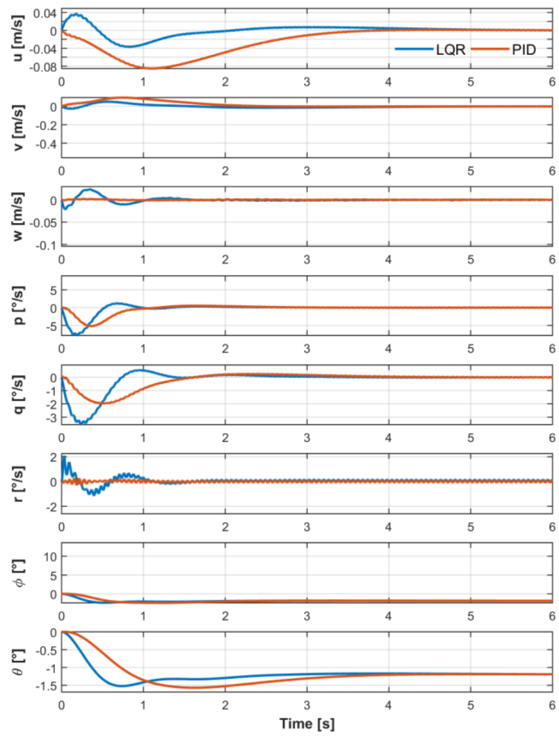

Figure 5: Response of the complete system in hover to a non-homogeneous initial condition; comparison of PID (red) and LQR (blue) performance.

equilibrium condition which is not null, whereas all rates are reduced to zero after a transient phase, as can be expected in a stable trimmed condition.
It can be observed from Figure 5 that both controllers offer a fast settling time, the duration of the transient phase being slightly higher for the LQR controller.

Table 1: Linear and angular speed residuals in a trimmed condition in hover for PID and LQR.

	PID	LQR
$\lvert\boldsymbol{\Delta V}\rvert$	9.6E-6	6.0E-5
$\lvert\boldsymbol{\Delta\omega}\rvert$	9.2E-3	6.6E-2

The norm of the residual of the linear and angular speeds after the transient – $\lvert\boldsymbol{\Delta V}\rvert$ and $\lvert\boldsymbol{\Delta\omega}\rvert$, respectively – can be used to check the distance of the final condition in the simulations shown in Figure 5 from an actual trim. The respective values obtained for the PID and LQR are reported in Table 1.

Notwithstanding the control reactivity witnessed by a lower settling time, the LQR is slightly less precise than the PID on the trimmed condition, but the error is generally very small in all cases.

3.2 Control in Forward Flight

As previously pointed out, in order to fully exploit the potential of the proposed linear design framework, it is necessary to have a linearized model parameterized in terms of the airspeed over the operating envelope of the helicopter. Provided no analytic model can be practically used to this end, an approach to model synthesis via parameter identification can be adopted instead.
The first step is that of finding a trimmed condition, in terms of inputs and attitude angles, to be used as a reference equilibrium condition for linearization. This can be done by using one of the control laws designed and tested in hover in an off-design condition, where the longitudinal speed will be not null. The intensity of the airspeed at which the controller designed for hover will still be capable of trimming the machine can be determined via a trial and error procedure considering a progressive longitudinal acceleration.
The PID and LQR controllers designed for hover have been preliminarily tested at airspeeds of 10 m/s and 20 m/s, yielding, as a side-product of the analysis, an assessment of the robustness of the respective control design approaches in off-design conditions. The values of the norms of the steady state errors are reported in Table 2.

Table 2: Linear and angular speed residuals in a trimmed condition in advanced flight (10-20 m/s) for PID and LQR.

	10 m/s		20 m/s	
	PID	LQR	PID	LQR
$\lvert\boldsymbol{\Delta V}\rvert$	5.0E-4	2.0E-5	(unstable)	2.5E-5
$\lvert\boldsymbol{\Delta\omega}\rvert$	2.6E-2	6.8E-2	(unstable)	3.7E-2

It can be noted from Table 2 that the LQR is capable of reducing the steady-state error on the linear speed more effectively than the PID at 10 m/s, whereas they are similarly capable of reducing the angular rates.

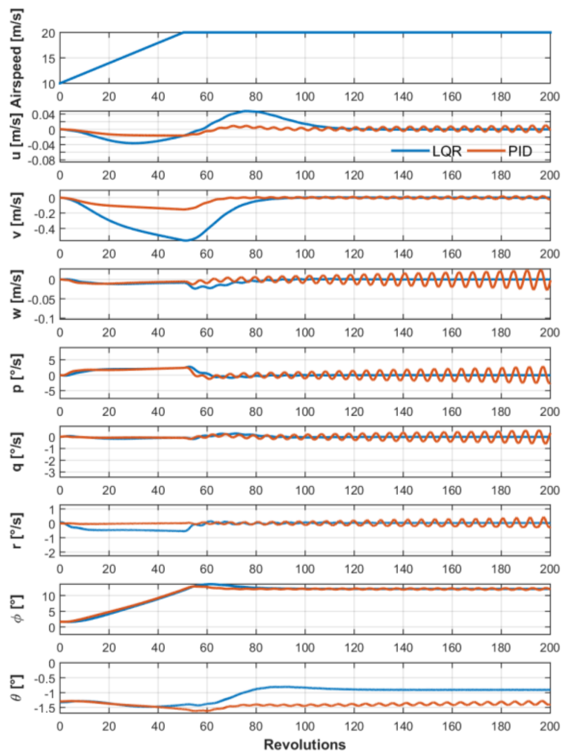

Figure 6: Response of the complete system during a time-linear transition from 10 m/s to 20 m/s. Comparison of PID and LQR performance.

The PID shows a lower degree of robustness with respect to the LQR, as can be noticed by the appearance of an instability such to hamper holding the machine in a trimmed condition steadily.

Figure 6 shows the result of a simulation where the longitudinal airspeed is increased from 10 m/s to 20 m/s with a time-linear ramp. From the plot it is apparent that a substantial instability shows up in case the PID is used, whereas the LQR proves capable of trimming the helicopter at the higher airspeed, even if with a partly degraded performance, as can be seen from the duration of the transient, longer than for simulations at lower speeds.

3.3 Model Identification

In order to check the feasibility of the proposed approach to the solution of the trim problem at higher airspeeds, the virtual model controlled with the LQR designed for hover on the analytic model was trimmed at 10 m/s and subjected to an exogenous input while under control of the trimmer. The PID was not considered in this phase, for its very structure is bound to the dynamics typical of hover – a limitation of this control technique. Several input time histories were considered preliminarily, based on several combinations of positive and negative steps on all four controls. A specific sequence of steps has been finally selected as a result of multiple identification trials.

The implemented PEM method for identification is based on an unconstrained minimization of the prediction error and a weight matrix computed on the covariance of the error obtained from the difference between the time histories of the output of the virtual plant and those of the analytic model for hover, integrated under the same conditions – i.e. controlled with the same gain matrix and subject to the same wind and exogenous input.

The PEM method has been initialized with the analytic model for hover. The prediction error is reduced to about 63% of its initial value as a result of parameter fitting. A comparison of the time histories of the states for the multi-body model, the analytic model for hover – initial condition of the identification method – and the new identified model is shown in Figure 7.

From Figure 8, the eigenvalues of the open loop system appear to have changed, especially roll, pitch and heave. In percentage, also the spiral mode has moved significantly towards stability. Nonetheless, the overall map of the eigenvalues has not been altered to a point such to result in a general behavior of the machine much different with respect to the hover condition.

With a new model successfully identified for 10 m/s, a new LQR gain matrix could be computed again based on the procedure presented in Section 2.2.2 with an optimal selection of the weighting matrix $\boldsymbol{Q}$.

In order to smooth transition between airspeeds, the optimal procedure was constrained in order to ensure reaching the same level of performance (specified in Section 2.2.1) on both the linearized model for hover and the new one for 10 m/s. The merit function was based only on the identified model. The resulting map of the eigenvalues is shown in Figure 9.

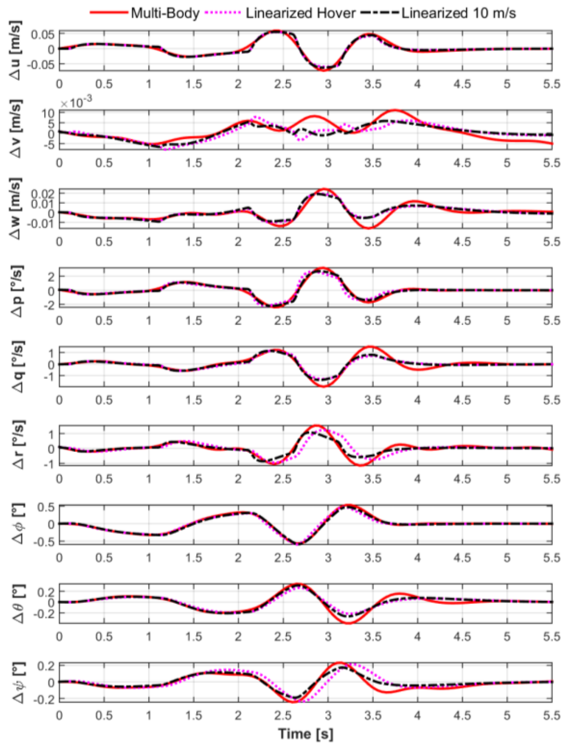

Figure 7: Comparison of the response of the closed loop system to an assigned control input for identification, in forward flight at 10 m/s; comparison of multi-body (ground truth, red), analytic model for hover (magenta) and identified model for 10 m/s (black).

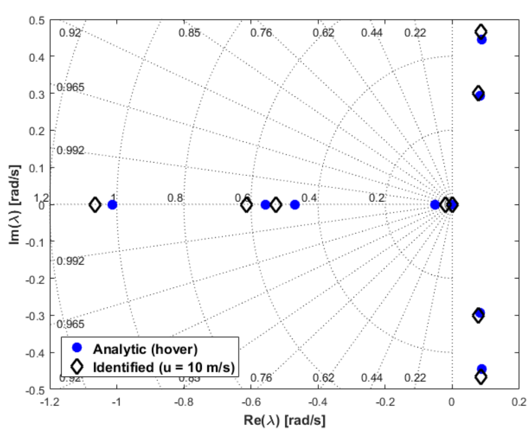

Figure 8: Comparison of the eigenvalues of the open-loop system, considering the analytic model for hover (blue) and the identified model for 10 m/s forward flight (black).

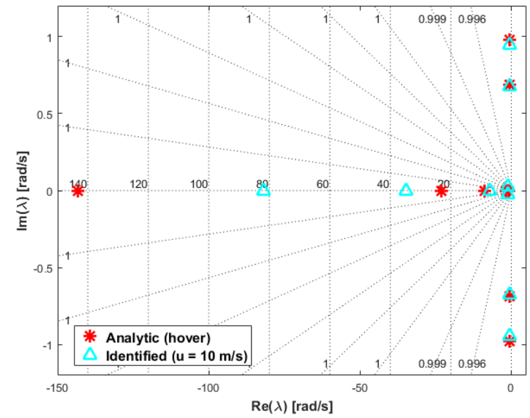

Figure 9: Comparison of the eigenvalues of the closed-loop systems, resulting from the application of an optimally tuned LQR to the analytic model for hover (red) and the identified model for 10 m/s forward flight (cyan).

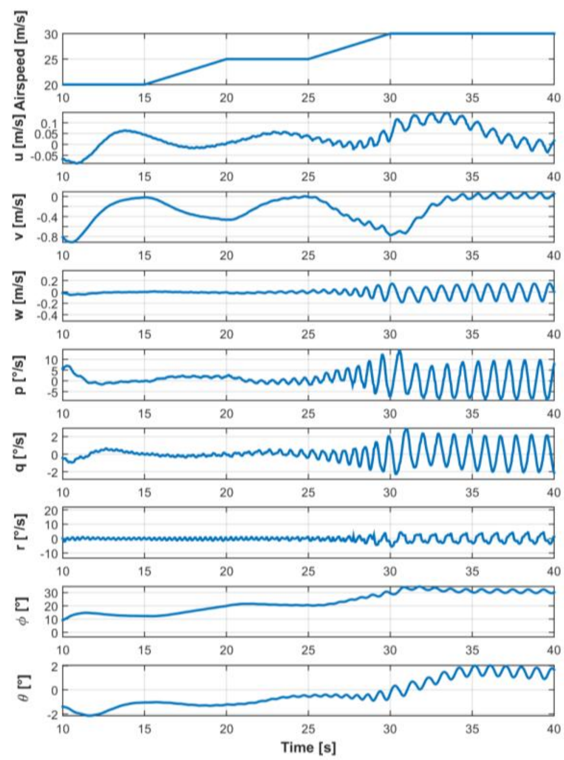

Figure 10: Testing the multi-body system in off-design conditions with an LQR controller designed on the model identified at 10 m/s.

Integrating the multi-body model under the same conditions considered for Figure 6 with the control gain matrix obtained from the identified model at 10 m/s leads to a time response extremely similar to that of Figure 6. Increasing the airspeed to 25 m/s, differently from the trimmer designed for hover, the new controller designed for 10 m/s succeeds in stabilizing the system, as shown in Figure 10. Further increasing the speed to 30 m/s the system is not yet unstable, but some significant oscillations show up.
This suggests that, in this region of the operating envelope, between almost-hover to sustained forward flight, linearized models should be identified at airspeed intervals of 10-15 m/s at most.

4 CONCLUSIONS

The use of a linear model of a rotorcraft for trimming purposes has been investigated. For hover, an analytic model has been prepared first. Based on it, a PID and an LQR controller have been assembled. Tuning has been performed using the linearized system to setup an optimal analysis. The performance of the trimmers has been assessed, and the LQR appears to allow deployment in slightly off-design conditions more robustly. A model for a higher airspeed has been identified from closed-loop simulations. A controller designed on the identified model has proved capable of trimming the rotorcraft at an airspeed higher than the maximum for which the controller based on the model for hover does. This, in turn, suggests that the control design procedure based on linearized model identification and control synthesis at progressively higher airspeeds should allow trimming the rotorcraft over its full operating envelope.

5 ACKNOWLEDGEMENTS

The contribution of the Master’s thesis student Davide Pinato in the preliminary investigation of some identification issues is gratefully acknowledged.

6 REFERENCES

[1] D. Peters, B. Kim and H. Chen, "Calculation of trim settings for a helicopter rotor by an optimized automatic controller," *Journal of Guidance, Control, and Dynamics,* vol. 7, no. 1, pp. 85-91, 1984.

[2] B. Ren, S. Ge, C. Chen, C. Fua and T. Lee, Modeling, Control and Coordination of Helicopter Systems, New York, NY: Springer, 2012.

[3] R. Prouty, Helicopter Performance, Stability, and Control, Malabar, FL: Krieger Publishing Company, 2002.

[4] A. Panza and M. Lovera, "“Rotor State Feedback in Rotorcraft Attitude Control," in *41st European Rotorcraft Forum*, Munich, Germany, 2015.

[5] G. Padfield, Helicopter Flight Dynamics: The Theory and Application of Flying Qualities and Simulation Modelling, Oxford: Blackwell, 2007.

[6] A. Visioli and M. Johnson, Practical PID Control: Advances in Industrial Control, London: Springer, 2006.

[7] M. Johnson, G. Chen, D. Greenwood, M. Grimble, S. Kwong, K. Man, P. Martin, M. Moradi, A. Sánchez, Q. Wang and Y. Zhang, PID Control, London: Springer, 2005.

[8] A. Bryson and Y. Ho, Applied Optimal Control: Optimization, Estimation, and Control, New York: Wiley, 1975.

[9] J. Morris, M. van Nieuwstadt and P. Bendotti, "Identification and Control of a Model Helicopter in Hover," in *Proceedings of the American Control Conference*, Baltimore, MD, 1994.

[10] D. Shim, H. Kim and S. Sastry, "Control System Design for Rotorcraft-Based Unmanned Aerial Vehicles Using Time-Domain System Identification," in *Proceedings of the 2000 IEEE International Conference on Control Applications*, Anchorage, AK, 2000.

[11] B. Kim, Y. Chang and M. Lee, "System Identification and 6-DOF Controller Design of Unmanned Model Helicopter," *JSME International Journal,* vol. 49, no. 4, pp. 1048-1057, 2006.

[12] A. Croce, R. Possamai, A. Savorani and L. Trainelli, "Modelling and Characterization of a Novel Gimbal Two-Blade Helicopter Rotor," in *40th European Rotorcraft Forum*, Southampton, UK,

2014.

[13] A. Croce, R. Possamai and L. Trainelli, "Dynamic Properties of Some Gimbal and Teetering Two-Blade Helicopter Rotor Heads," in *40th European Rotorcraft Forum*, Southampton, UK, 2014.

[14] L. Trainelli, A. Croce, C.E.D. Riboldi, R. Possamai and A. Castagnoli, "Multibody Modelling of a Novel Two-Bladed Helicopter: Trim Studies," in *ECCOMAS Thematic Conference on Multibody Dynamics*, Barcelona, Spain, 2015.

[15] L. Trainelli, A. Croce, C.E.D. Riboldi and R. Possamai, "Trimming a High-Fidelity Multibody Helicopter Model for Performance and Control Analysis," in *41st European Rotorcraft Forum*, Munich, Germany, 2015.

[16] O. Bauchau, C.L. Bottasso and Y. Nikishkov, "Modeling Rotorcraft Dynamics with Finite Element Multibody Procedures," *Mathematics and Computer Modeling,* vol. 33, pp. 1113-1137, 2001.